

---

## STUDY OF FUNDAMENTAL PROPERTIES OF COVZ (Z= P, BI, SB AND AS) HALF HEUSLER COMPOUNDS

Pardeep Kumar Jangra<sup>a, b</sup>, Anshul Singh<sup>a</sup> Ajay Singh Verma<sup>c</sup>, Sukhender<sup>d,\*</sup> Praveen Kumar<sup>e</sup> Anita Kumari<sup>f</sup>

<sup>a</sup>Department of Chemistry, B. M. U. Asthal Bohar( Rohtak)

<sup>b</sup>Department of Chemistry, G. C. W. Badhra (Charkhi Dadri)

<sup>c</sup>Division of Research and Innovation, Uttranchal University (Dehradun)

<sup>d</sup>Department of Physics, GDC Memorial College, Bahal (Bhiwani)

<sup>e</sup>Department of Physics, G. C. W. Tosham (Bhiwani)

<sup>f</sup>Department of Physics, S.V. College, Raja Mahendra Pratap Singh State University, Aligarh

\*Corresponding author

Using first principle techniques, the structural, electrical, elastic, and magnetic properties of Half-Heusler CoVZ (Z= P, Bi, Sb, and As) compounds with the space group F-43<sub>m</sub> have been examined. Here, we employ the WIEN2k-implemented full potential linearized augmented plane wave (FP-LAPW) technique. The compounds CoVZ (Z= P, Bi, Sb, and As) exhibit 100% spin polarization with a finite band gap of 0.61, 0.67, 0.65, and 0.68 eV, respectively, close to the Fermi level as implemented in the WIEN2k algorithm. It is discovered that these substances are semiconducting in nature. These compounds, CoVZ (Z= P, Bi, Sb, and As), have estimated magnetic moments of 1.31, 1.35, 1.27, and 1.20  $\mu_B$ . Here, we note that the Slater-Pauling rule and the code's computed results have excellent tuning. We conclude from the study that all compounds are ductile, with the exception of CoVGe, which exhibits brittle nature. A positive value of Cauchy pressure ( $C_P = C_{12} - C_{44}$ ) indicates ductile nature of material, whereas a negative result demonstrates brittle nature of material. Cauchy pressure and Pugh's ratio both display the same kind of outcome. With the exception of CoVAs, which is almost ductile, all of these compounds' elastic characteristics demonstrate that they are ductile. Whereas other CoVAs have metal character, which can also be anticipated by their small band gaps, the Poisson ratio of CoVAs indicates covalent character. Materials can be compared based on their hardness by being arranged in decreasing order, for example, CoVAs > CoVSb > CoVP > CoVBi. The sole mechanically unstable alloy in this class is CoVBi, whereas CoVSb is the hardest and brittlest material.

**Keywords:** Spintronics, Semiconducting, Band gap, Density of State, Magnetic Moment

### Introduction

At the Isabellenhütte in 1901, Dr. Friedrich Heusler created a novel class of materials [1]. He has created synthetic samples of the three non-magnetic metals: tin, manganese, and copper. He observed that the alloy consisting of one part manganese and one part aluminium, with two parts copper, has high ferromagnetic characteristics [2-3]. Heusler compounds are ternary intermetallic materials consisting of a main group component and two transition metal atoms. Four face-

centered cubic sub lattices are present in Heusler and half-Heusler chemically formed materials  $X_2YZ$ , while compounds with formula  $XYZ$  comprise three FCC sublattice interpenetrates [4–7]. The Neel temperature of 550C for antiferromagnetic CuMnSb was predicted by Keizo Endo et al. [8] using R. H. Forster's observed lattice parameter and interpretation based on theory of resonance scattering [9]. K. Watanabe et al. [10] investigated the magnetic properties of Mn-based half-Heusler compounds and came to the conclusion that the number of valence electrons affects the magnetic interaction of such compounds in solid solutions. The Clb compounds with six valence electrons per unit formula [11] had a gradual decrease in Curie temperature as the Mn-Mn distance increased, but for seven valence electron count as this distance increases, a transition from antiferromagnetic to weak ferromagnetism occurs. A noteworthy characteristic of Mn-based Clb Heusler structure compounds was discovered in 1983 by R.A. de Groot et al. [12]. They employed scalar relativistic effects in their augmented spherical wave approach [13–14]. According to G.L. Bona et al. [15], NiMnSb exhibits ferromagnetic half-metallicity. According to the results of spin-polarized photoemission techniques, there is no observation of 100% polarisation near the photo-Threshold from the spin component.

### Computational Details

First principle calculations are performed using the full potential Linearized Augmented Plane Wave (FP-LAPW) approach provided in the WIEN2k simulation package [16–17] to describe the interaction between atomic core and valence electrons. The valence electrons are taken into consideration when extending the electronic wave function. At Perdew-Burke-Ernzerhof (PBE), the energy of exchange-correlation is defined using the generalized gradient approximation (GGA) [18–19]. We employed the spin-polarized Density Functional Theory's (SDFT) FP-LAPW approach to optimize the shape of the electronic structure. In order to extend the spherical harmonics in the atomic sphere, the value of  $l_{max}$  is assumed to be 6. Up to  $G_{max}=12$ , the charge density and potential in the middle region were produced as Fourier series with a wave vector. According to the alloys examined, Table 1 provides the muffin-Tin radii of each atomic sphere [20].  $RMT \times K_{max}$  is the convergence criterion that LAPW employs.

**Table 1**

To avoid overlapping spheres during the SCF cycle, the Muffin-Tin Radii of each atomic sphere for the optimized lattice parameter of each specific alloy are shown.

Compounds	Atoms	RMT
CoVP	Co	2.16
	V	2.08
	P	1.79
CoVAs	Co	2.21
	V	2.12
	As	2.12
CoVSb	Co	2.34

	<b>V</b>	2.22
	<b>Sb</b>	2.36
<b>CoVBi</b>	<b>Co</b>	1.89
	<b>V</b>	1.89
	<b>Bi</b>	2.04

We have fixed the energy between these two states at -6.0Ry. Relativistic core states and semi-relativistic valence states are distinguished. The SCF cycle is considered to have converged when, between successive iterations, the energy difference and the integration of the absolute charge density difference are fewer than 10<sup>-5</sup>Ry and 0.001 Coulomb/formula unit, respectively. Wien2k keeps the overall K-point count for irreducible Brillouin zones at 1000. Based on ab initio total-energy or stress computations, ElaStic\_1.0 is used to compute the full second-order elastic stiffness tensor for crystal structures. The maximum absolute value of Lagrangian strain is 0.5, and the number of deformed strain structures is fixed at 11.

### Results and Discussion

The lattice parameters are calculated and the minimum energy for the previously specified substances is measured in the first stage. One can derive the equilibrium lattice parameters by minimizing the energy in relation to the volume.

#### Structural Properties:

Half-Heusler compounds crystallise in the face-centered cubic with space group F-43<sub>m</sub> and structurbericht designation C1b. These compounds can be understood as follows: V and Z in CoVZ compounds, Y and Z in MnXY compounds at (1/2,1/2,1/2) position, and Mn with Ru, Fe, Ni, and Pd create zinc blend sublattice organized in a primitive cell at Wyckoff positions (0, 0, 0) and (1/4,1/4,1/4). Volume optimization was carried out using the Murnaghan equation, which describes the energy and pressure values as a function of volume and can be applied to any feasible configuration of each component [21–23]:

$$E(V) = E_0 + \left[ \frac{BV}{B_P} \left( \frac{1}{(B_P-1)} \left( \frac{V_0}{V} \right)^{B_P} + 1 \right) - \frac{BV_0}{(B_P-1)} \right] \quad (1)$$

$$P(V) = \frac{B}{B_P} \left\{ \left( \frac{V_0}{V} \right)^{B_P} - 1 \right\} \quad (2)$$

The volume vs. energy curves is shown in Figure1. For further studies, only that arrangement which has minimum energy and electro negativity order is to be considered [24-27].

**Table 2**

For each arrangement, electro negativity and energy for CoVPb tabulated in table 2 and 3

Elements	Electronegativity
<b>Co</b>	01.88
<b>V</b>	01.63
<b>Bi</b>	02.02

<b>P</b>	02.19
<b>As</b>	02.18
<b>Sb</b>	02.05

**Table 3**

Measured values of band gap, equilibrium volume and minimum energy for type I, II and III structural configuration

Compound	Structural configuration	Energy (Ry)	Equilibrium Volume (a.u. <sup>3</sup> )	BAND Gap (eV)
<b>CoVP</b>	Type I	-5367.87	270.53	0
	Type II	-5367.83	277.77	0
	Type III	-5367.64	262.88	0.60
<b>CoVAs</b>	Type I	-9208.77	297.79	0
	Type II	-9208.76	306.83	0
	Type III	-9208.19	287.96	0.71
<b>CoVSb</b>	Type I	-17649.75	371.03	0
	Type II	-17649.79	380.68	0
	Type III	-17649.07	333.94	0.68
<b>CoVBi</b>	Type I	-47849.49	398.94	0
	Type II	-47849.56	390.43	0
	Type III	-47849.47	362.79	0.71

**Table 4**

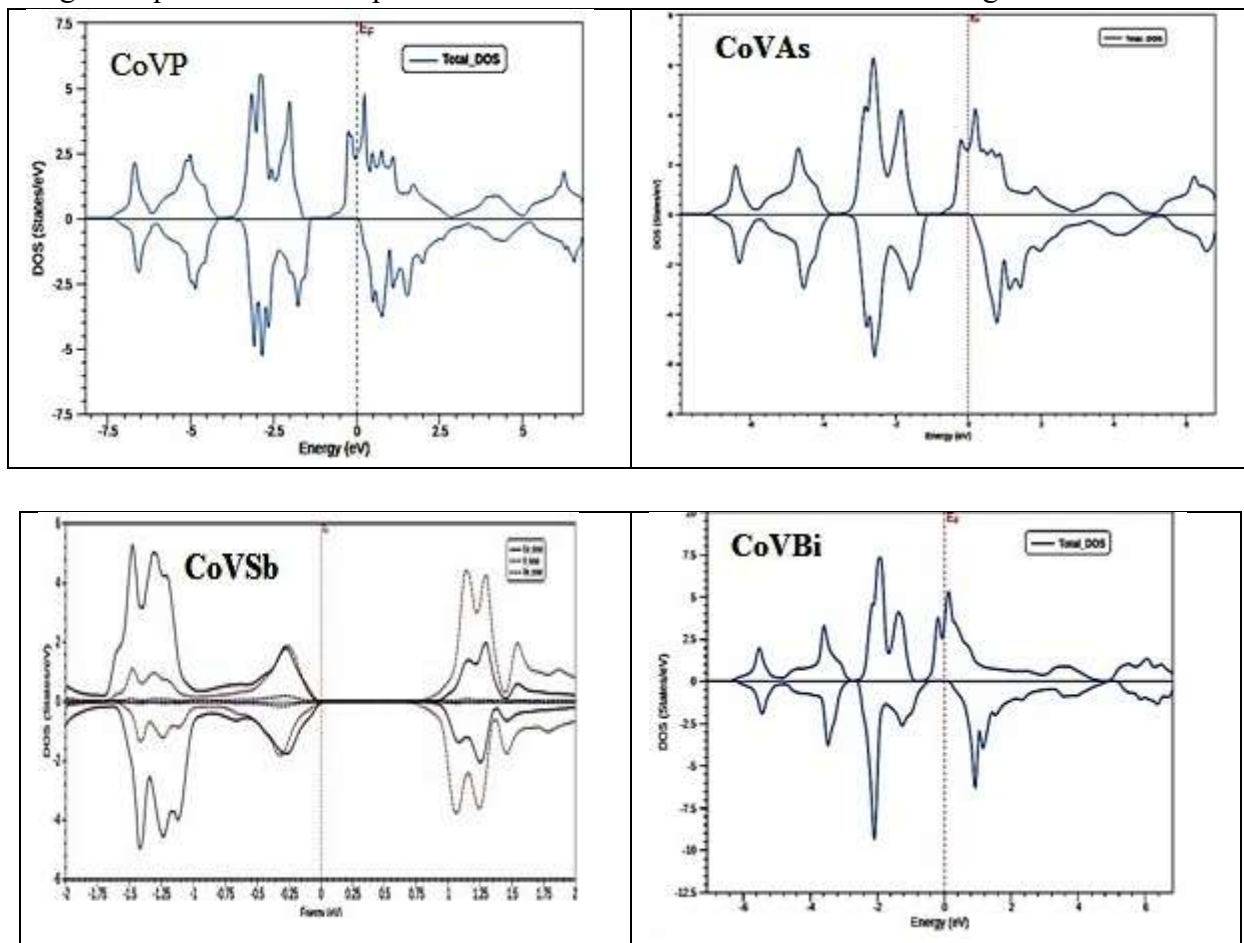
Observed values of the lattice parameter (a<sub>0</sub>), equilibrium volume, bulk modulus (B), pressure derivative of bulk modulus (BP) and minimum energy during optimization

Compound	Optimized Lattice Parameter (Å)	Equilibrium Volume (a.u. <sup>3</sup> )	Bulk Modulus (GPa)	B.P	Energy (Ry)
<b>CoVP</b>	4.41	262.88	201.15	6.47	-5367.64
<b>CoVAs</b>	4.55	287.96	172.04	4.93	-9208.19
<b>CoVSb</b>	4.79	333.94	142.07	4.51	-17649.07
<b>CoVBi</b>	4.95	362.79	121.19	4.59	-47849.47

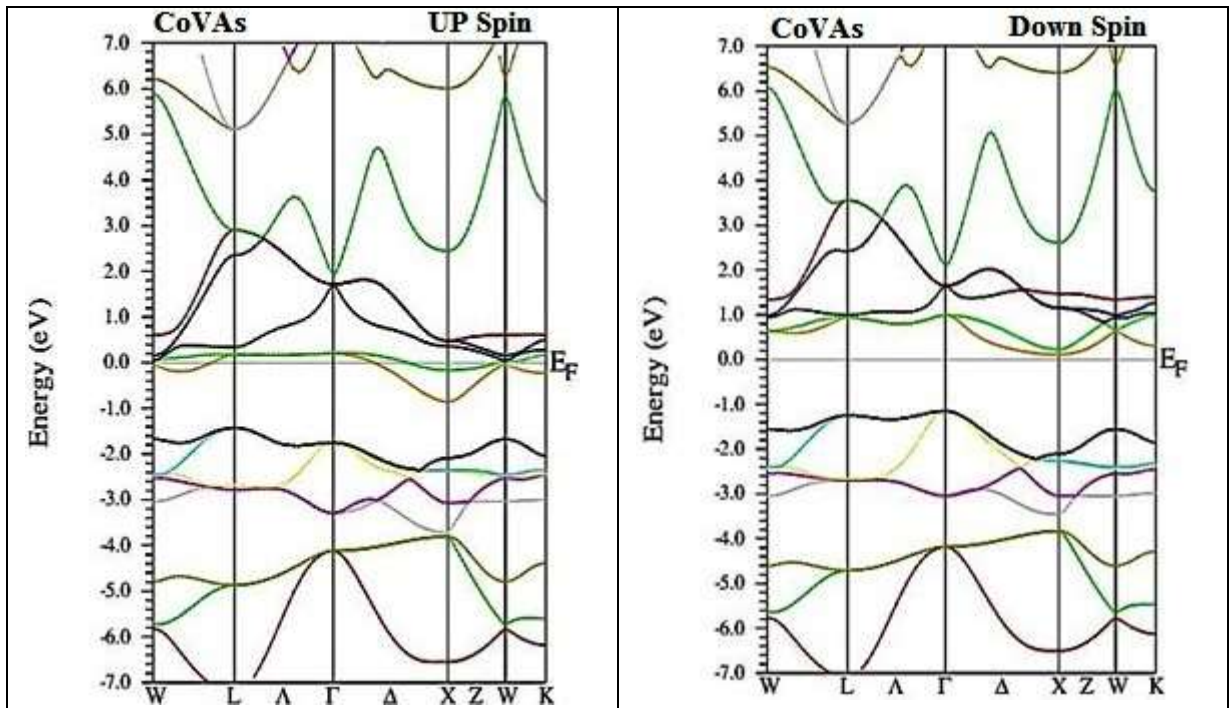
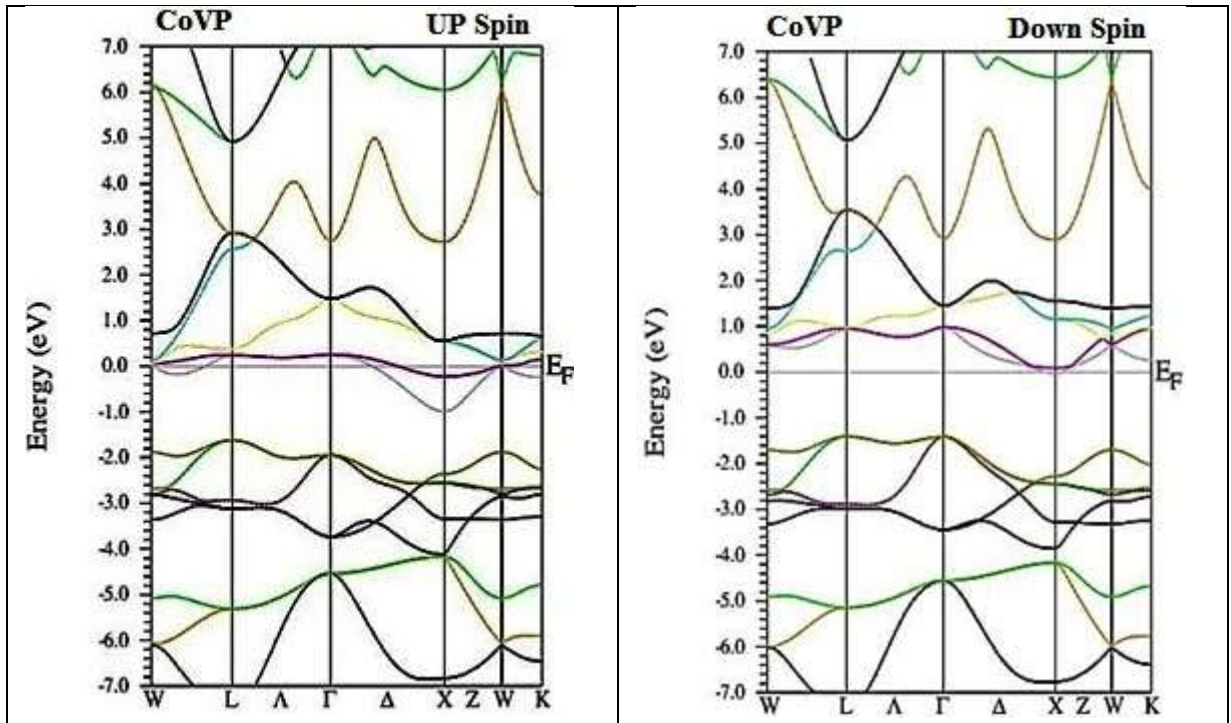
### Electronic Properties

We first examine the full DOS configuration of each chemical in order to analyze the electrical structure of all alloys. 3-d metal atom states, which vary from -0.5 to + 4.3 eV, hybridize with one another in partial DOS, as shown in Figure below. This is because the half-metallic band difference

in some compounds is a significant factor. The density of state allows for the investigation of the CoVZ chemical bonding property. The hybridization between the d-states of Co and V is the primary mechanism of the chemical bond, as can be seen from the partial densities of the figure below. A chemical bond can be both covalent and ionic at the same time. Covalent because both transition elements' d states are strongly hybridized and degenerate over a large portion of their extension, and ionic because the relative quantities of Co and V's 3-d states differ below and above the Fermi point, favoring V's 3-d states. Moreover, the compounds CoVZ (Z= P, Bi, Sb, and As) contain 19 valence electrons. The semi-metallic behavior of half-Heusler materials can be identified in large part by looking at the electronic structure. We also computed the total DOS using the equilibrium lattice parameter in order to examine the electrical image of these materials.



**Figure 1:** Total density of states of all the compounds at their equilibrium lattice constant



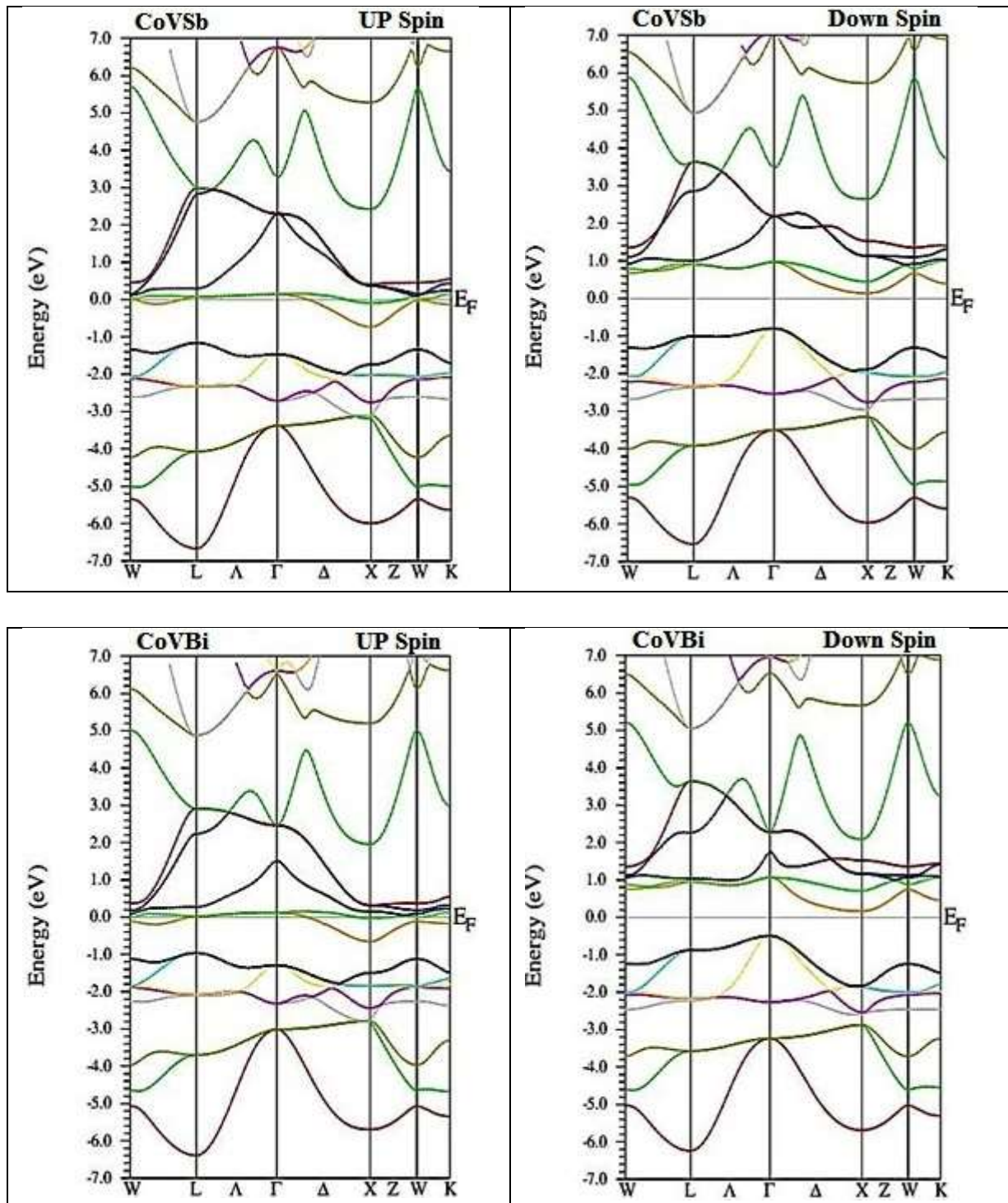


Figure 2: The Band Structure of the Compounds CoVP, CoVAs, CoVSb and CoVBi

**Table 5**

Total band gap and band transition between special points of first Brillion zone

Compound	$E_g$ (eV)	BAND Transition	Compound	$E_g$ (eV)	BAND Transition
CoVP	0.61	W→X	CoVAs	0.67	L→X
CoVSb	0.65	L→X	CoVBi	0.68	L→X

### Magnetic properties

By calculating the difference between the up and down spin states, the Galanakis model determines the spin magnetic moment of these materials [28–30]. The peculiar behavior of half metallic ferromagnetism is explained by the underlying magnetic moment, which for these compounds obeys the Slater-Pauling rule as illustrated below.

$$M_{\uparrow} = Z_{\uparrow} - 18;$$

Where  $M_{\uparrow}$ : total magnetic moment/ f.u and

$Z_{\uparrow}$ : total number of valence electrons.

For example, Co, V, P, Bi, Sb and As atoms have 9, 5, 5, 5, 5 and 5 valence electrons counts.

**Table 6**

Total Magnetic Moment Per Formula Unit of the Compounds CoVP, CoVAs, CoVSb and CoVBi

Compound	Total Magnetic Moment Per Formula ( $\mu_B$ )
CoVP	1.31
CoVAs	1.35
CoVSb	1.27
CoVBi	1.20

In addition, the spin polarization P is defined by

$$P = \frac{n_{\uparrow} - n_{\downarrow}}{n_{\uparrow} + n_{\downarrow}} \times 100\%$$

Where,  $n_{\uparrow}(E_f)$  and  $n_{\downarrow}(E_f)$  are the spin-dependent density of states around the Fermi level.

The table below lists the total magnetic moment and valence electron count for each formula unit [31–34]. The compounds with 18 valence electrons are obviously completely spin polarized. The estimated result is in good accord with the magnetic moment's theoretical value [35].



**Table 7**

Theoretical values of Magnetic Moment according to the Slater-Pauling rule and their corresponding Spin Polarizing nature

Compound	$Z_t$	$M_t$ ( $\mu_B$ )	Spin Polarization
CoVP	19	1	100%
CoVAs	19	1	100%
CoVSb	19	1	100%
CoVBi	19	1	100%

### Mechanical Properties

Elastic constant is used to analyze hardness, stress, and all pressure-induced structural deformations. The Poisson ration effect, Young's modulus, shear modulus, Debye temperature, and melting temperature of solids are all studied with great importance because to these constants. For cubic crystal, there are only three different elastic constants:  $C_{11}$ ,  $C_{12}$ , and  $C_{44}$ . The elastic constant tensors (in Voigt notation) arising from the alteration in internal energy deformation are represented by the  $C_{ij}$  in this instance [36–38]. The shear modulus considers the solid's resistance to shear deformation-preserving volume, while the bulk modulus  $B$  describes the solid's resistance to volume change.

In the study and creation of materials, elastic structures are important. Taylor's expansion of the elastic energy or stress in terms of the applied strain characterizes elastic tensors of any order. It is necessary to determine the three second-order elastic constants (SOEC),  $C_{11}$ ,  $C_{12}$ , and  $C_{44}$ , in order to characterize the dynamic and mechanical behavior of the alloys under study. There are only three different elastic constants for cubic crystal formations, according to Hooke's law:  $C_{11}$ ,  $C_{12}$ , and  $C_{44}$ .  $C_{11}=C_{22}=C_{33}$ ,  $C_{12}=C_{13}=C_{23}$ , and  $C_{44}=C_{55}=C_{66}$  are the results of the symmetry of the second-order elastic constant matrix in Voigt notation. The compound's stability is confirmed by the fact that none of the elastic constant matrix's Eigen values are zero. Aside from this requirement, the Born's theory-based stability criteria are as follows:  $C_{11}>0$ ,  $C_{44}>0$ ,  $C_{11}>|C_{12}|$ , and  $(C_{11}+2C_{12})>0$ .

The researched XYZ compounds are mechanically stable because the elastic constants of the cubic crystals are thought to be compatible with the aforementioned stability requirements [39].

**Table 8**

Elastic constants of half-Heusler compounds in the units of GPa

Compounds	C <sub>11</sub>	C <sub>12</sub>	C <sub>44</sub>	Compounds	C <sub>11</sub>	C <sub>12</sub>	C <sub>44</sub>
CoVP	267.4	154.4	74.4	CoVSb	313.5	64.0	79.6
CoVAs	313.6	64.2	79.3	CoVBi	136.4	139.2	59.7

**Table 9**

Elastic properties of half-Heusler compounds having 19 valence electron calculated

Compounds	CoVP	CoVAs	CoVSb
<b>B<sub>V</sub>= B<sub>R</sub>= B<sub>H</sub></b>	192.14	147.07	147.07
<b>G<sub>V</sub></b>	67.86	97.5	97.5
<b>G<sub>R</sub></b>	66.54	92.90	92.90
<b>G<sub>H</sub></b>	67.21	94.30	94.30
<b>E<sub>V</sub></b>	182.2	239.81	239.81
<b>E<sub>R</sub></b>	178.96	230.40	230.40
<b>E<sub>H</sub></b>	180.58	234.16	234.16
<b>η<sub>V</sub></b>	0.34	0.21	0.21
<b>η<sub>R</sub></b>	0.34	0.22	0.22
<b>η<sub>H</sub></b>	0.34	0.24	0.24
<b>B<sub>H</sub>/G<sub>H</sub></b>	2.86	1.56	1.56

**Table 10**

Values of Zener anisotropy index (A), degree of elastic anisotropy in percentage (A\*), Kleinman parameter (ζ), Lamé's coefficient (λ), Pugh ratio (K) and Vickers hardness of material having half-Heusler compounds having 19 valence electron

Compounds	CoVP	CoVAs	CoVSb
A	1.34	0.64	0.64
A*(%)	1.01	2.42	2.42
Z	0.69	0.36	0.36
$\Lambda$	154.23	63.98	63.98
K	0.35	0.65	0.65
Hv	0.86	11.28	11.28

With the exception of CoVAs, which is almost ductile, all of these compounds' elastic characteristics demonstrate that they are ductile. Whereas other CoVAs have metal character, which can also be anticipated by their small band gaps, the Poisson ratio of CoVAs indicates covalent character. Materials can be compared based on their hardness by being arranged in decreasing order, for example, CoVAs > CoVSb > CoVP > CoVBi. The average wave velocities that are compressed and stretched are also used to compute Debye's temperature. Compounds with 19 valance electrons are half-metallic in minority band, fermi level is close to conduction band. CoVSb is the hardest and brittle materials where as CoVBi is the only mechanically unstable alloy in this category.

### Conclusions

The compounds CoVP, CoVAs, CoVSb, and CoVBi exhibit semiconducting behavior with finite band gaps of 0.61, 0.67, 0.65, and 0.68 eV, respectively, according to the results of the research of these properties. These compounds, CoVZ (Z= P, Bi, Sb, and As), have estimated magnetic moments of 1.31, 1.35, 1.27, and 1.20  $\mu$ B. These findings demonstrate that the estimated magnetic moment agrees well with the behavior of Slater-Pauling. With the exception of CoVAs, which is almost ductile, all of these compounds' elastic characteristics demonstrate that they are ductile. Materials can be compared based on their hardness by being arranged in decreasing order, for example, CoVAs > CoVSb > CoVP > CoVBi. The sole mechanically unstable alloy in this class is CoVBi, whereas CoVSb is the hardest and brittlest material.

### References

- [1] Dr. Fr. Heusler, Dr. E. Take, The nature of the heusler alloys, Trans. Faraday Soc. **8** (1912) 169-184.

- [2] J. Li, Y. Li, G. Zhou, Y. Sun, and C. Q. Sun, A first Principles study on the full Heusler compound  $\text{Cr}_2\text{MnAl}$ , *Appl. Phys. Lett.* **94**(2009), 242502
- [3] F. Casper, T. Graf, S. Chadov, B. Balke and C. Felser, Half- Heusler compounds: novel materials for energy and spintronic applications, *Semicond. Sci. Technol.* **27** (2012) 063001.
- [4] R.A. De Groot, F.M. Muller, P.G. Van Engen and K.H.J. Buschow, New class of materials: half-metallic ferromagnets, *Phys. Rev. Lett.* **50** (1983) 2024-2027.
- [5] S. A. Khandya , I. Islamb , D. C. Gupta and A. Laref, Full Heusler alloys ( $\text{Co}_2\text{TaSi}$  and  $\text{Co}_2\text{TaGe}$ ) as potential spintronic materials with tunable band profiles, *J. Solid State Chem.*, **270** (2019) 173-179.
- [6] T. Graf, C. Felser and S. S.P. Parkin, Simple rules for the understanding of Heusler compounds, *Prog. Solid State Chem.* **39** (2011) 1-50.
- [7] C. Felser, L. Wollmann, S. Chadov, G. H. Fecher, and S. S. P. Parkin, Basics and prospective of magnetic Heusler Compounds, *APL Mater.* **3** (2015) 041518.
- [8] K. Endo, Magnetic Studies of Clb-Compounds  $\text{CuMnSb}$ ,  $\text{PdMnSb}$  and  $\text{Cu}_{1-x}(\text{Ni or Pd})_x\text{MnSb}$ . *J. Phys. Soc. Jpn.* **29**, 643 (1970).
- [9] J. Friedel, The use of positrons for the study of solids. *Nuovo Cimento* **7** (1958) 287.
- [10] K. Watanabe, Magnetic Properties of Clb-Type Mn Base Compounds. *Trans. Jpn. Inst. Met.* **17**, 220 (1976).
- [11] G. Mima, *Kinzokusoshikigaku (Metallography)*, Asakurasyoten, (1960) 600.
- [12] R.A. de Groot, F.M. Mueller, P.G. van Engen, K.H.J. Buschow. New class of materials: half-metallic ferromagnets. *Phys. Rev. Lett.* **50**, 2024 (1983).
- [13] A. R. Williams, J. Kubler, and C. D. Gelatt, Jr., Cohesive properties of metallic compounds: Augmented-spherical-wave calculations. *Phys. Rev. B* **19**, 6094 (1979).
- [14] M. Methfessel and J. Kübler, Bond analysis of heats of formation: application to some group VIII and IB hydrides. *J. Phys. F* **12**, 141 (1982).
- [15] G.L. Bona, F. Meier, M. Taborelli, E. Bucher, P.H. Schmidt, Spin polarized photoemission from  $\text{NiMnSb}$ . *Solid State Commun.* **56**, 391(1985).
- [16] Y. Miura, K. Nagao and M. Shirai, Atomic disorder effects on half-metallicity of the full-Heusler alloys  $\text{Co}_2(\text{Cr}_{1-x}\text{Fe}_x)\text{Al}$ : A first-principles study, *Phys. Rev. B* **69** (2004) 144413.
- [17] J. Kübler, G. H. Fecher, C. Felser, Understanding the trend in the Curie temperatures of  $\text{Co}_2$ - based Heusler compounds: Ab initio calculations. *Phys. Rev. B* **76** (2007) 024414
- [18] S. A. Wolf, D. D. Awschalom, R. A. Buhrman, J. M. Daughton, S. V. Molnar, M. L. Roukes, A. Y. Chtchelkanova, D. M. Treger, Spintronics: a spin-based electronics vision for the future, *Science*, **294** (2001) 1488-1495.
- [19] E. Şaşıoğlu, L. M. Sandratskii, P. Bruno, I. Galanakis, Exchange Interactions and Temperature Dependence of Magnetization in half-Metallic Heusler Alloys, *Phys.*

- Rev. B., 72 (2005) 184415.
- [20] S. Wurmehl, G. H. Fechel, H. C. Kandpal, V. Ksenofontov, C. Felser, H. Lin, Investigation of Co<sub>2</sub>FeSi: The Heusler compound with highest Curie temperature and magnetic moment, *Appl. Phys. Lett.*, 88 (2006) 032503.
- [21] Sukhender, Lalit Mohan, Sudesh Kumar, Deepak Sharma, Ajay Singh Verma, Structural, electronic, optical and magnetic properties of Co<sub>2</sub>CrZ (Z= Al, Bi, Ge, Si) Heusler compounds, *East Eur. J. Phys.* 2 (2020) 69-80. <https://doi.org/10.26565/2312-4334-2020-2-05>
- [22] Sukhender, Pravesh Pravesh, Lalit Mohan, Ajay Singh Verma, Ductile and metallic nature of Co<sub>2</sub>VZ (Z= Pb, Si, Sn) Heusler compounds: a first principles study, *East Eur. J. Phys.*, 3 (2020) 99-110. <https://doi.org/10.26565/2312-4334-2020-3-13>
- [23] Sukhender, Pravesh Pravesh, Lalit Mohan, Ajay Singh Verma, First principles calculations for electronic, optical and magnetic properties of full heusler compounds, *East Eur. J. Phys.* 3 (2020) 111-121. <https://doi.org/10.26565/2312-4334-2020-3-14>
- [24] Sukhender, Lalit Mohan, Ajay Singh Verma, Electronic, optical, elastic and magnetic properties of Co<sub>2</sub>VZ (Z= As, B, In, Sb) Heusler compounds, *East Eur. J. Phys.*, 4 (2020) 51-62. <https://doi.org/10.26565/2312-4334-2020-4-07>
- [25] F. Gregor, K. Perter, Ternary semiconductors NiZrSn and CoZrBi with half-Heusler structure: A first-principles study. *Phys. Rev. B.* 94 (2016) 075203.
- [26] C. K. Barman, A. Alam, Topological phase transition in the ternary half-Heusler alloy ZrIrBi. *Phys. Rev. B.* 97 (2018) 075302.
- [27] S. Ishida, S. Akazawa, Y. Kubo, J. Ishida, Band theory of Co<sub>2</sub>MnSn, Co<sub>2</sub>TiSn and Co<sub>2</sub>TiAl, *J. Phys. F: Met. Phys.* 12 (1982) 1111.
- [28] J. Kübler, A.R. William, C.B. Sommers, Formation and coupling of magnetic moments in Heusler alloys. *Phys. Rev. B* 28 (1983) 1745-1755.
- [29] A. Sozinov, A.A. Likhochev, N. Lanska and Ullakko. Giant magnetic-field-induced strain in NiMnGa seven-layered martensitic phase. *Appl. Phys. Lett.*, 80 (2002) 1746.
- [30] J. Marcos, L. Manosa, A. Planes, F. Casanova, X. Batlle, and A. Labarta. Multiscale origin of the magnetocaloric effect in Ni-Mn-Ga shape-memory alloys. *Phys. Rev. B*, 68 (2003) 094401.
- [31] A. Planes, L. Manosa and M. Acet. Magnetocaloric effect and its relation to shape-memory properties in ferromagnetic Heusler alloys. *J. Phys., Condens. Matter* 21, 233201 (2009).
- [32] A. N. Vasil'ev. Shape memory ferromagnets. *Phys.-Usp.* 46 (2003) 559.
- [33] J. Pons, E. Cesari, C. Segn, F. Masdeu, R. Santamarta. Ferromagnetic shape memory alloys: Alternatives to NiMnGa. *Mat. Sci. Eng.*, 57 (2008) A 481482.
- [34] C. M. Fang, G. A. d. Wijs and R. A. d. Groot, Spin-polarization in half-metals (invited), *J. Appl. Phys.* 91(2002) 8340-8344.
- [35] M. Bowen, A. Barthélémy, M. Bibes, E. Jacquet, J. P. Contour, A. Fert, D. Wortmann and S. Blügel, Half-metallicity proven using fully spin-polarized tunnelling, *J. Phys., Condens.*

Matter, 17 (2005) 407.

- [36] R. J. Soulen, J. M. Byers, M. S. Osofsky, B. Nadgorny, T. Ambrose, S. F. Cheng, P. R. Broussard, C. T. Tanaka, J. Nowak, J. S. Moodera, A. Barry and J. M. D. Coey, Measuring the spin polarization of a metal with a superconducting point contact, *Science*, 282 (1998) 85-88.
- [37] J. C. Slater, The Ferromagnetism of Nickel, *Phys. Rev.* 49 (1936) 537-545.
- [38] L. Pauling, The Nature of the Interatomic Forces in Metals, *Phys. Rev.* 54 (1938) 899-904.
- [39] H. Ohno, A window on the future of spintronics, *Nature Materials*, 9 (2010) 952-954.